Hindawi
Advances in Mathematical Physics
Volume 2020, Article ID 6721909, 8 pages
https://doi.org/10.1155/2020/6721909

Research Article

PSO–SOM Neural Network Algorithm for Series Arc Fault Detection

Na Qu,[1] **Jiatong Chen**,[2] **Jiankai Zuo**,[3] **and Jinhai Liu**[4]

[1]*School of Safety Engineering, Shenyang Aerospace University, Shenyang 110136, China*
[2]*School of Aviation Engine, Shenyang Aerospace University, Shenyang 110136, China*
[3]*School of Computer Science, Shenyang Aerospace University, Shenyang 110136, China*
[4]*School of Information Science and Engineering, Northeastern University, Shenyang 110004, China*

Correspondence should be addressed to Na Qu; 11502332@qq.com

Received 22 June 2019; Revised 5 September 2019; Accepted 17 September 2019; Published 25 January 2020

Academic Editor: Emilio Turco

Self-organizing feature map (SOM) neural network is a kind of competitive neural network with unsupervised learning. It has the strong abilities of self-organization and self-learning. However, the classification accuracy of SOM neural network may decrease when the features of tested object are not obvious. In this paper, the particle swarm optimization (PSO) algorithm is used to optimize the weight values of SOM network. Three indexes, *i.e.,* intra-class density, standard deviation and sample difference, are used to judge the weight value, which can improve the classification accuracy of the SOM network. PSO–SOM network is applied to the detection of series arc fault in electrical circuits and compared with conventional SOM network and learning vector quantization (LVQ) network. The detection accuracy of the PSO–SOM network is 95%, which is higher than conventional SOM network and LVQ network.

1. Introduction

In the low voltage supply environment, the insulation ability of electrical wires or appliances will decline because of the aged or damaged insulation layer. When the voltage reaches a certain value, an arc fault may occur. When a series arc fault occurs, the current value is often less than the threshold of the circuit breaker. But its temperature can reach to thousands of degrees and it is not easily extinguished. While maintaining voltage is 20 V, the arc can still maintain a continuous and stable combustion. It is easy to cause the electrical fire. Statistical analysis shows that the proportion of electric fires caused by arc faults is up to 50%. Therefore, the detection of series arc fault is meaningful to ensure electrical safety.

The research of arc fault detection mainly focuses on arc simulation model, current feature extraction and detection algorithm. Cassie and Mayr models are proposed early [1, 2]. The Cassie arc model is mainly used for large current periods before current crosses zero. The Mayr arc model is mainly used for small current periods when the current crosses zero. On the basis of Cassie model and Mayr model, Habedank model [3], modified Mayr model [4], Schwamaker model [5], segmented arc model [6–9] and so on, have been proposed. Current feature extraction mainly includes time domain feature extraction and frequency domain feature extraction. The time domain feature is mainly based on the zero-rest phenomenon of arc fault current [10]. The frequency domain feature extraction is mainly based on Fourier transform [11–13] and wavelet transform [14–16]. The detection algorithms mainly include neural network [17, 18], support vector machine (SVM) [19, 20], Chirp-zeta transform [21], matrix coefficients [22], quantum probability mode [23] etc. Neural network, SVM, and Chirp-zeta transform are often used in indoor power distribution system. Matrix coefficients method are suitable for circuit with few load types, mainly used for aircraft arc fault detection. Quantum probability model is mainly applied to arc fault detection of photovoltaic power generation system.

In this paper, the particle swarm optimization (PSO) algorithm is used to optimize self-organizing feature map (SOM) neural network. Three indexes, *i.e.,* intra-class density, standard deviation and sample difference, are used to judge the weight value, which can improve the classification accuracy of the SOM network. PSO–SOM algorithm is applied to the

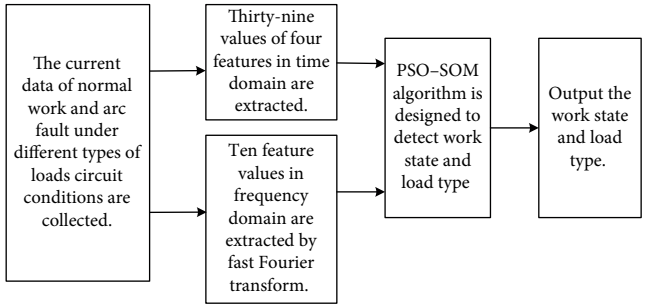

Figure 1: The block diagram of complete description.

Table 1: Load type and sampling resistance.

Load type	Load name	Sampling resistance
Resistive and inductive load	Lamp and inductor in series	100 Ω
Resistive load	Lamp	100 Ω
Eddy current load	Induction cooker	1 Ω
Switching power supply load	Computer	50 Ω
Series motor load	Hand drill	50 Ω

detection of series arc fault in electrical circuits and compared with conventional SOM network and learning vector quantization (LVQ) network. The block diagram of complete description is shown as Figure 1.

2. Current Features Extraction

The current is selected as the detection signal and the current data are collected by arc fault experiment platform. The experimental platform is mainly composed of power supply, arc generator, loads, and acquisition device. The power supply is 220 V and 50 Hz AC. Arc generator is mainly composed of fixing carbon electrode and moving copper electrode. TDS1001C-SC of Tektronix oscilloscope and TPP0101 10X of voltage probe are selected to collect data. The current data are obtained by the sampling resistance method. The sampling resistance method is to connect a resistor in series in the circuit and measure the voltage across the resistor, then use Ohm's law to get the current. The sample data come from five types of load circuits, as shown in Table 1. The current features are extracted from both time domain and frequency domain.

2.1. Features Extraction in Frequency Domain. The fast Fourier transform (FFT) is used to obtain the current amplitude spectrum. The amplitudes of 0~2000 Hz are selected for features extraction. The frequency range is divided into ten intervals on average. The mean current amplitude of each interval is calculated as one feature value in the frequency domain, and there are ten feature values in total.

A set of feature values under the conditions of lamp and inductor in series load, lamp load, induction cooker load, computer load, and hand drill load are shown in Tables 2–6.

It can be seen from Tables 2–6 that the amplitudes of fault current are higher than those of normal current when the loads are lamp and inductor in series, lamp and computer. The amplitudes of fault current are lower than those of normal current in low frequency band and higher than those of normal current in high frequency band when the load is induction cooker. The amplitude difference between fault current and normal current is not obvious when the load is hand drill.

Table 2: Frequency domain feature values of lamp and inductor in series load circuit.

Load name	Mean amplitude of fault current (%)	Mean amplitude of normal current (%)	Frequency range/Hz
Lamp and inductor in series	0.0318	0.0194	0–200
	0.0124	0.0005	200–400
	0.0129	0.0007	400–600
	0.0120	0.0015	600–800
	0.0115	0.0007	800–1000
	0.0108	0.0014	1000–1200
	0.0106	0.0010	1200–1400
	0.0078	0.0016	1400–1600
	0.0082	0.0011	1600–1800
	0.0064	0.0009	1800–2000

Table 3: Frequency domain feature values of lamp load circuit.

Load name	Mean amplitude of fault current (%)	Mean amplitude of normal current (%)	Frequency range/Hz
Lamp	3.7304	2.9273	0–200
	0.9459	0.0210	200–400
	0.5663	0.0911	400–600
	0.4564	0.0758	600–800
	0.2605	0.0204	800–1000
	0.2916	0.0973	1000–1200
	0.2300	0.0542	1200–1400
	0.1797	0.0569	1400–1600
	0.2215	0.0611	1600–1800
	0.1782	0.0290	1800–2000

Table 4: Frequency domain feature values of induction cooker load circuit.

Load name	Mean amplitude of fault current (%)	Mean amplitude of normal current (%)	Frequency range/Hz
Induction cooker	0.1383	1.7710	0–200
	0.0500	0.2482	200–400
	0.1131	1.4436	400–600
	0.0774	0.2819	600–800
	0.0480	0.0533	800–1000
	0.1119	0.1298	1000–1200
	0.0723	0.0539	1200–1400
	0.0664	0.0306	1400–1600
	0.0748	0.0353	1600–1800
	0.0660	0.0349	1800–2000

Table 5: Frequency domain feature values of computer load circuit.

Load name	Mean amplitude of fault current (%)	Mean amplitude of normal current (%)	Frequency range/Hz
Computer	0.6353	0.0197	0–200
	0.7551	0.0033	200–400
	0.6838	0.0026	400–600
	0.6898	0.0019	600–800
	0.7297	0.0012	800–1000
	0.7902	0.0006	1000–1200
	0.5011	0.0016	1200–1400
	0.6562	0.0011	1400–1600
	0.6743	0.0016	1600–1800
	0.6181	0.0006	1800–2000

Table 6: Frequency domain feature values of hand drill load circuit.

Load name	Mean amplitude of fault current (%)	Mean amplitude of normal current (%)	Frequency range/Hz
Hand drill	15.4219	16.3304	0–200
	0.2571	0.3504	200–400
	0.3232	0.3253	400–600
	0.1677	0.1674	600–800
	0.0714	0.0574	800–1000
	0.0894	0.1255	1000–1200
	0.0704	0.0567	1200–1400
	0.0569	0.0773	1400–1600
	0.1135	0.0937	1600–1800
	0.0552	0.0640	1800–2000

2.2. Features Extraction in Time Domain. In the time domain, one cycle of current is divided into ten segments on average. Four features of current, *i.e.*, current average, current pole difference, current variance and current difference average, are calculated. The current average, current pole difference, and current variance respectively correspond to one number in each segment and ten numbers in one cycle. The difference average contains nine numbers in one cycle, because it is obtained by calculating the current difference between two adjacent segments. Thirty-nine numbers are obtained as current features in time domain.

The experimental data of five types of load circuit current are measured and the induction cooker load circuit current is taken as an example to illustrate features extraction, as shown in Figure 2. There are obvious differences between fault current and normal current.

3. PSO–SOM Algorithm for Arc Fault Detection

In order to improve the classification accuracy, the PSO is used to optimize the weight values of SOM [24–26]. PSO–SOM is applied to the detection of series arc fault in different load circuits. Three indexes, *i.e.*, intra-class density, standard deviation and sample difference, are used to judge the weight value.

3.1. SOM Neural Network. SOM neural network is a kind of competitive neural network with unsupervised learning. It has the strong ability of self-organization and wide applications in classification problem. The network structure consists of input layer and competition layer. The input layer corresponds to a group of high-dimensional input vectors. The competition layer consists of ordered nodes in two-dimensional grid. The input vectors and output nodes are connected by weight vectors.

The learning steps of SOM neural network are as follows:

(a) Initialize the network structure, the neuron numbers each layer, and the weight values.

(b) Input the training samples and use Equation (1) to calculate the Euclidean Distances between the weight vector and the input vector.

$$d_j = \sqrt{\sum_{i=1}^{m} \left(x_i - w_{ij}\right)^2}, \tag{1}$$

where x_i represents the i^{th} input vector, w_{ij} represents the weight vector between the j^{th} neuron of competitive layer and the i^{th} neuron of input layer, m represents the number of input layer neurons.

(c) The neuron with the minimum Euclidean distance in the competitive layer is the winning neuron. Update neuron weight vectors within a certain distance around the winning neuron, as (2).

$$w_{\text{new}} = w_{\text{old}} + \eta(i)\left(x_i - w_{ij}\right), \tag{2}$$

where w_{new} and w_{old} represent the weight vectors of updated and before update, respectively. Here, $\eta(i)$ represents learning rate varying with training frequency and is determined by (3).

$$\eta(i) = r_{\max} - \frac{i}{maxgen}\left(r_{\max} - r_{\min}\right), \tag{3}$$

where $r_{\max}$ is the maximum of learning rate, $r_{\min}$ is minimum of learning rate, and $maxgen$ is the maximum of training steps.

The radius of the weight update range is determined by (4).

$$l = l_{\max} - \frac{i}{maxgen}\left(l_{\max} - l_{\min}\right), \tag{4}$$

where $l_{\min}$ is the minimum of dynamic radius, $l_{\max}$ is the maximum of dynamic radius.

(d) After the training of the network, the test sample is input into the network. The winning neuron is the category of detection result.

3.2. PSO Algorithm. PSO is a swarm intelligence optimization algorithm and the purpose is to solve the optimal value by imitating the movement rule of birds in the process of

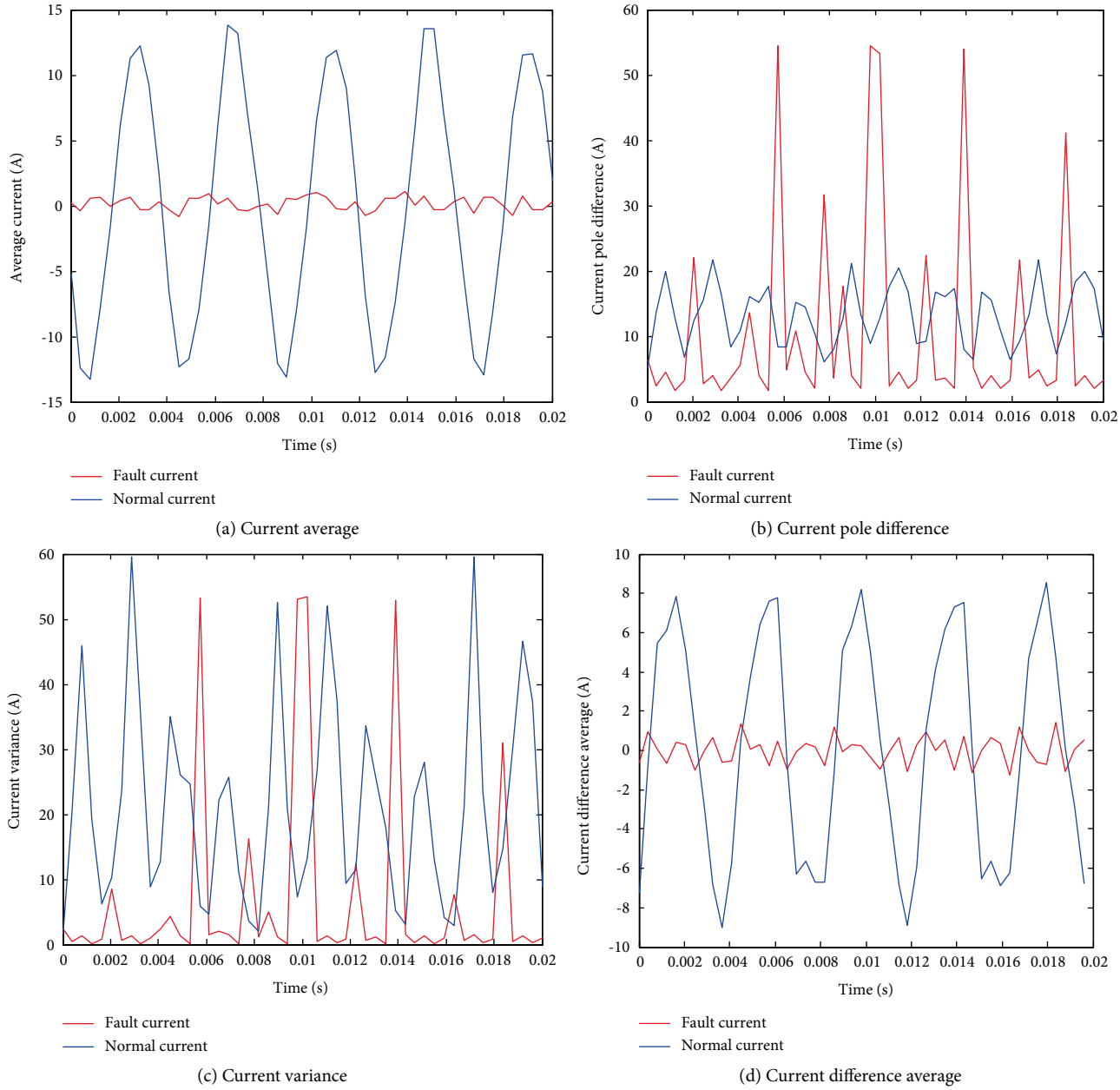

Figure 2: The time domain features extraction of induction cooker load circuit.

predation. The main training process of the PSO algorithm is as follows.

(a) Determine the fitness function and generate a certain number of particles in the feasible domain. Each particle is a potential optimal solution.

(b) Calculate the each particle value according to the fitness function, and select the individual and group extreme value. Then update the position and speed of all particles according to (5) and (6).

$$V_{k+1} = \omega V_k + c_1 a_1 (P_i - X) + c_2 a_2 (P_g - X), \quad (5)$$

$$X_{k+1} = X_k + V_{k+1}, \quad (6)$$

where V_k is the speed of the particle in the last iteration, V_{k+1} is the speed after this update. P_i is the individual extreme value of the particle and P_g is population extreme value of the particle. c_1 and c_2 are nonnegative constants and take 1.5 here. r_1 and r_2 are random numbers between 0 and 1. X_k is the position of particle before updated, X_{k+1} is the position of particle after updated.

(c) Repeat the calculation process of the second step until all particles converge to a certain point which is the optimal value.

3.3. PSO–SOM Algorithm Design. The PSO algorithm is used to optimize the weight values of SOM network. Three

indexes, *i.e.,* intra-class density, standard deviation and sample difference, are used to judge the weight value, which can improve the classification accuracy of the SOM network.

(a) *Intra-Class Density.* Intra-class density is used to measure the aggregation degree of the same category of data, as shown in (7).

$$D = \sum_{j=1}^{p} \sum_{i=1}^{n} \left(R - \alpha_{ij}\right) f\left(R - \alpha_{ij}\right), \tag{7}$$

where R is the window width parameter and takes 0.1 here, α_{ij} is the Euclidean distance between the weight vector and input vector, f is the step function and takes 1 when the independent variables is greater than or equal to 0, or takes 0.

(b) *Standard Deviation.* The standard deviation is used to measure the dispersion degree of data, as shown in (8).

$$S = \sqrt{\frac{\sum_{i=1}^{n} \left(v_i - v_{ave}\right)^2}{n-1}}, \tag{8}$$

where v_i is the weight vector of the i^{th} neuron, v_{ave} is the average vector value, n is the number of competing neurons.

(c) *Sample Difference.* Sample difference is used to measure the similarity degree among the same category of neurons, as shown in (9).

$$L = \sum_{i=1}^{n} \min\left(dist\left(v_i, v_{data}\right)\right), \tag{9}$$

where $\min\left(dist\left(v_i, v_{data}\right)\right)$ is the minimum of the Euclidean distance of the i^{th} neuron weight vector.

The fitness function of PSO algorithm is obtained by using the above three indexes, as shown in (10).

$$y = \frac{SD}{L}. \tag{10}$$

The PSO–SOM algorithm flow chart is shown in Figure 3.

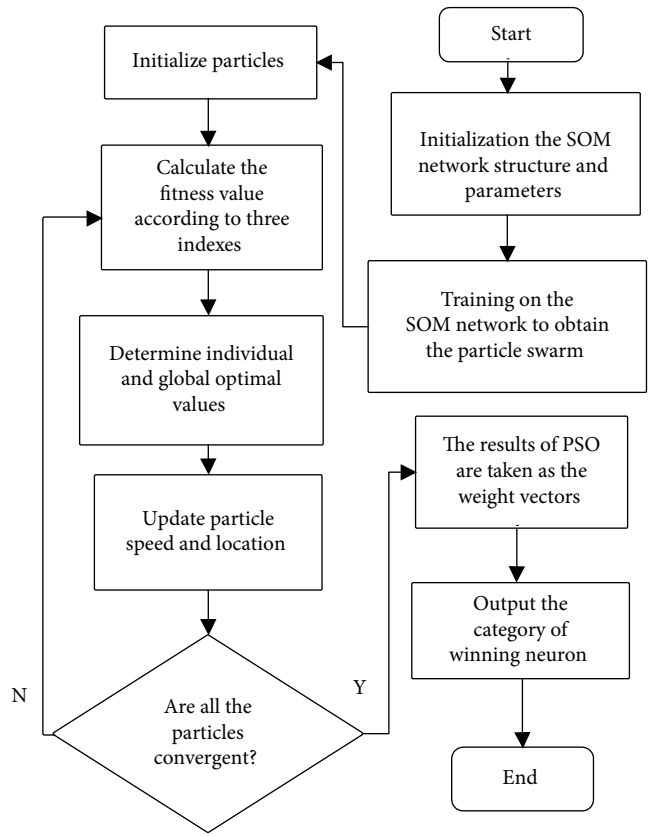

Figure 3: The flow chart of PSO–SOM algorithm.

3.4. Arc Fault Detection. The PSO–SOM algorithm is used to establish the arc fault detection model [27–30]. The model inputs are forty-nine in total, including thirty-nine feature values in the time domain and ten feature values in the frequency domain. The outputs are ten kinds of states, *i.e.,* fault or normal state of lamp and inductor in series load, fault or normal state of lamp load, fault or normal state of induction cooker load, fault or normal state of computer load, fault or normal state of hand drill load, as shown in Table 7. Ten kinds of work states are numbered. The binary encoding method is adopted, and the encoding length is 4 bits. The first three bits represent the type of load and the last bit represents normal state or fault state.

The PSO–SOM model needs to cluster ten categories of samples. Each category takes 100 groups of samples. Among them, 60 groups of samples are selected as training data randomly, and the remaining 40 groups of samples as testing data. Then, there are 400 groups of samples as testing data in total.

Table 7: Load corresponding number in different working conditions.

Load type	Work state	Corresponding number
Lamp and inductor in series	Fault	0010
	Normal	0011
Lamp	Fault	0100
	Normal	0101
Induction cooker	Fault	0110
	Normal	0111
Computer	Fault	1000
	Normal	1001
Hand drill	Fault	1010
	Normal	1011

In addition, other parameters of PSO–SOM model are set [31, 32]. In the SOM network, the number of competing neurons is $6 \times 6 = 36$, the maximum of the network learning rate is 0.2, the minimum is 0.05, the maximum and minimum of the weight update radius is 1.5 and 0.8, the training steps are 200. In the PSO algorithm, the swarm size is 10, the maximum of individual speed is 0.5, the individual position coordinate range is ±2, the maximum of training steps is 100.

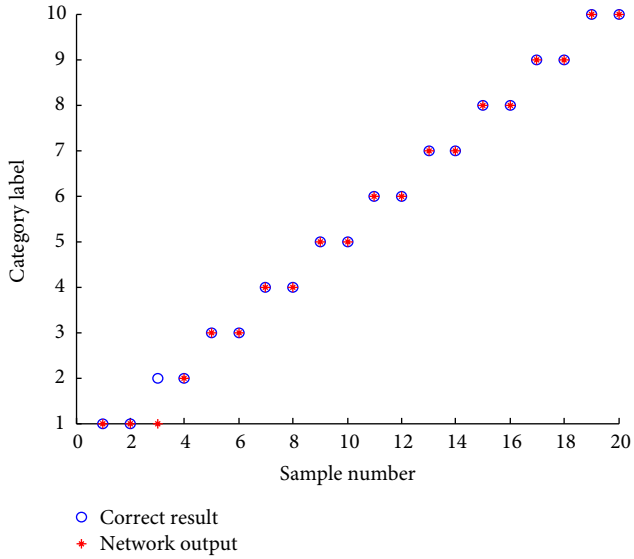

Figure 4: Detection results of PSO–SOM mode.

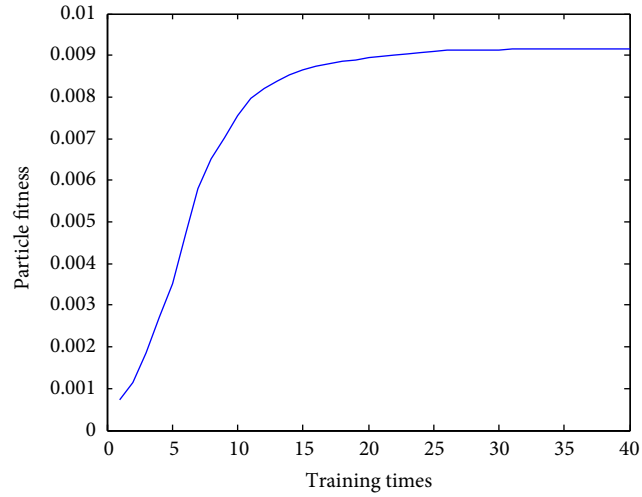

Figure 5: The optimization process of PSO algorithm.

Here, twenty groups of detection results are selected for demonstration, as shown in Figure 4. The horizontal axis represents the sample number, and the number 1–2 represents the fault state sample of lamp and inductor in series load, the number 3–4 represents the normal state sample of lamp and inductor in series load, the number 5–6 represents the fault state sample of lamp load, the number 7–8 represents the normal state sample of lamp load, the number 9–10 represents the fault state sample of hand drill load, the number 11–12 represents the normal state sample of hand drill load, the number 13–14 represents the fault state sample of computer load, the number 15–16 represents the normal state sample of computer load, the number 17–18 represents the fault state sample of induction cooker load, the number 19–20 represents the normal state sample of induction cooker load. The vertical axis represents the category. The blue circle indicates the correct category and the red asterisk indicates the detection result. If the two symbols coincide in the same category, the detection result is right. Otherwise, the detection result is wrong. It can be seen that there are nineteen results are correct, and only one result is wrong when the work state is normal state of lamp and inductor in series load.

The optimization process of the PSO algorithm is shown in Figure 5. The horizontal axis represents the training times and the vertical axis represents the particle fitness. It can be seen that all particles converge to the optimum fitness value of 0.0092 after 25 times of training.

4. Comparison with the Conventional SOM Network and LVQ Network Algorithms

Arc fault detection of PSO–SOM network is compared with conventional SOM network and LVQ network. The LVQ is a kind of competitive neural network with supervised learning. The LVQ network consists of input layer, hidden layer, and output layer. The main steps of LVQ network are as follows.

(1) Initialize the connection weight vectors and other parameters.

(2) Calculate the Euclidean distance between the weight vectors and the input vectors, as (11).

$$L = \sqrt{\sum_{i=1}^{m} \left(x_i - w_{ij}\right)^2}, \tag{11}$$

where x_i represents the i^{th} input vector, w_{ij} represents the weight vector between the j^{th} neuron of hidden layer and the i^{th} neuron of input layer, m represents the number of input layer neurons.

(3) If the category of output layer neuron according to the nearest neuron is the same as actual category of data, the weight vectors between hidden layer and input layer are modified according to (12).

$$w_{\text{new}} = w_{\text{old}} + \eta(x - w_{\text{old}}). \tag{12}$$

Otherwise, the weight vectors are modified according to (13).

$$w_{\text{new}} = w_{\text{old}} - \eta(x - w_{\text{old}}), \tag{13}$$

where w_{new} and w_{old} respectively represent the corrected weight and the weight before correction, η represents the learning rate.

Twenty groups of detection results of LVQ network are selected for demonstration, as shown in Figure 6. Twenty groups of detection results of conventional SOM network are selected for demonstration, as shown in Figure 7.

Four hundred groups of testing samples are input into PSO–SOM network, conventional SOM network, and LVQ network, respectively. The detection results are counted in Table 8. The detection accuracy of the PSO–SOM network is 95%, while those of the conventional SOM network and LVQ network are 56% and 53.25%. It shows the effectiveness of the LVQ network algorithm.

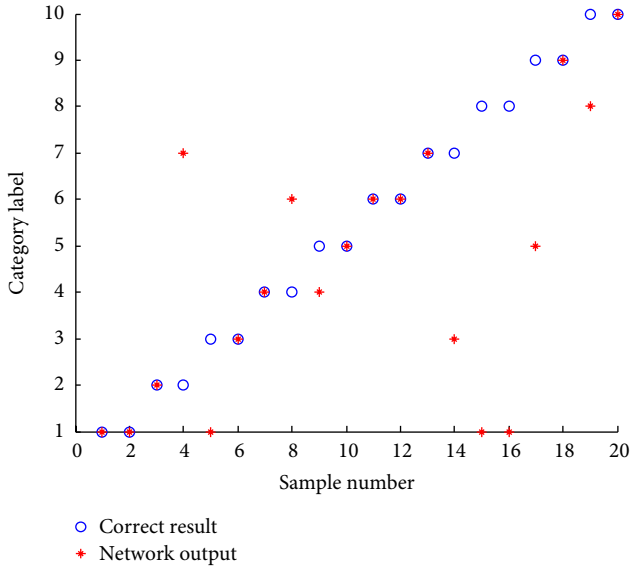

Figure 6: Detection results of LVQ network.

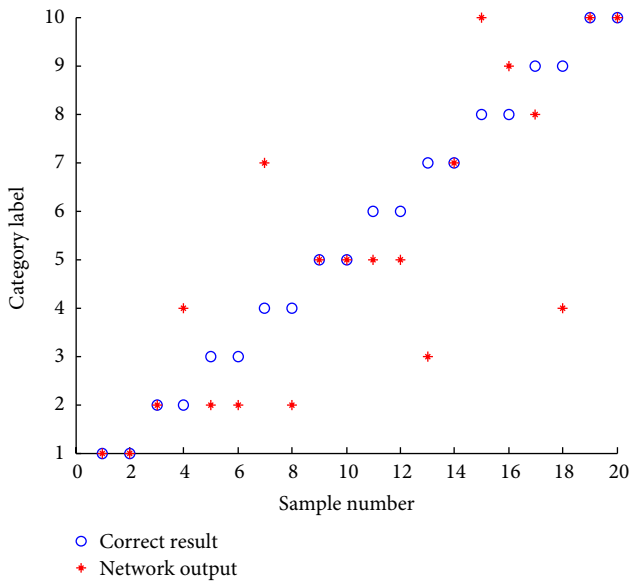

Figure 7: Detection results of conventional SOM network.

Table 8: Detection result comparison.

Algorithm	Number of test samples	Number of correct results	Detection accuracy (%)
LVQ network	400	213	53.25
SOM network	400	224	56
PSO–SOM network	400	380	95

5. Conclusions

In this paper, PSO algorithm is used to optimize the weight values of SOM network and three indexes, *i.e.,* intra-class density, standard deviation and sample difference, are used to judge the weight value. PSO–SOM network is applied to the detection of series arc fault in electrical circuits. The current is selected as the detection signal of arc fault. The current features are extracted from both time domain and frequency domain. Forty-nine feature values are taken as inputs of PSO–SOM model. Ten kinds of work states are taken as outputs of PSO–SOM model. The detection accuracy of the PSO–SOM network model is about 95%, which is higher than that of conventional SOM network model and LVQ network model.

Data Availability

The simulation data used to support the findings of this study are available from the corresponding author upon request.

Conflicts of Interest

The authors declare that they have no conflicts of interest.

Acknowledgments

This work was supported by the National Natural Science Foundation of China (61901283) and Department of Education Project of Liaoning Province (L201742).

References

[1] J. L. Guardado, S. G. Maximov, E. Melgoza, J. L. Naredo, and P. Moreno, "An improved arc model before current zero based on the combined Mayr and Cassie arc models," *IEEE Transactions on Power Delivery*, vol. 20, no. 1, pp. 138–142, 2005.

[2] A. Khakpour, S. Franke, S. Gortschakow, D. Uhrlandt, R. Methling, and K.-D. Weltmann, "An improved arc model based on the arc diameter," *IEEE Transactions on Power Delivery*, vol. 31, no. 3, pp. 1335–1341, 2016.

[3] U. Habedank, "Application of a new arc model for the evaluation of short-circuit breaking tests," *IEEE Transactions on Power Delivery*, vol. 8, no. 4, pp. 1921–1925, 1993.

[4] K. Qiao, W. Z. Liu, and J. Zhang, "Simulation of off-line arc simulation of bow network based on improved Mayr mode," *Railway Standard Design*, vol. 62, no. 5, pp. 138–142, 2018.

[5] P. H. Schavemaker and L. van der Slui, "An improved Mayr-type arc model based on current-zero measurements," *IEEE Transactions on Power Delivery*, vol. 15, no. 2, pp. 580–584, 2000.

[6] R. Hu, "Research on the influence of different arc models on circuits," *Northeast Electric Power Technology*, vol. 39, no. 5, pp. 18–20, 2018.

[7] Q. Wang, Z. Ye, and W. J. Tan, "Simulation and analysis of precise breakdown arc model," *Journal of Modern Power System and Clean Energy*, vol. 31, no. 10, pp. 4–9, 2015.

[8] T. Yan, W. H. Wu, and C. H. Xu, "Calculation and analysis of VFTO under trapezoidal dynamic arc model," *Electric Porcelain Arrester*, vol. 4, no. 12, pp. 188–193, 2018.

[9] Q. L. Wang, B. W. Wang, and H. L. Guan, "Model and experiment of low voltage AC series fault arc," *Journal of Electric Power System and Automation*, vol. 30, no. 2, pp. 26–30, 2018.

[10] Q. F. Yu, "Research on electrical fire forecast system and its application based on wavelet analysis and data fusion. Qinhuangdao [Ph.D.] dissertation," Department of Electrical Engineering Yanshan University, Qinhuangdao, China, 2013.

[11] P. Qi, S. Jovanovic, J. Lezama, and P. Schweitzer, "Discrete wavelet transform optimal parameters estimation for arc fault detection in low-voltage residential power networks," *Electric Power Systems Research*, vol. 143, pp. 130–139, 2017.

[12] K. Koziy, B. Gou, and J. Aslakson, "A low-cost power-quality meter with series arc-fault detection capability for smart grid," *IEEE Transactions on Power Delivery*, vol. 28, no. 3, pp. 1584–1591, 2013.

[13] L. Kumpulainen, G. A. Hussain, M. Lehtonen, and J. A. Kay, "Preemptive arc fault detection techniques in switchgear and controlgear," *IEEE Transactions on Industry Applications*, vol. 49, no. 4, pp. 1911–1919, 2013.

[14] R. Grassetti, R. Ottoboni, M. Rossi, and S. Toscani, "Low cost arc fault detection in aerospace applications," *IEEE Instrumentation & Measurement Magazine*, vol. 16, no. 5, pp. 37–42, 2013.

[15] J. P. Wang and H. Han, "New type of series arc model and characteristic analysis," *Electrical and Electronics*, vol. 12, pp. 33–36, 2017.

[16] S. Li, "Study of low cost arc fault circuit interrupter based on MCU," *International Journal of Control and Automation*, vol. 8, no. 10, pp. 25–34, 2015.

[17] R. Shi, J. Peng, and T. Wang, "Fault diagnosis of single-phase reclosing based on wavelet energy spectrum analysis in transmission line," *Journal of Xi'an Polytechnic University*, vol. 31, no. 6, pp. 788–794, 2017.

[18] X. Y. Yang, *Arc Fault Circuit Breaker*, University of Technology, Shenyang, 2018.

[19] Z. J. Wang, F. Zhang, S. W. Zhang, H.-Y. Gu, and P.L. Cao, "Series arc fault recognition method based on support vector machine approach," *Electrical Measurement & Instrumentation*, vol. 50, no. 4, pp. 22–26, 2013.

[20] S. H. Mortazavi, Z. Moravej, and S. M. Shahrtash, "A hybrid method for arcing faults detection in large distribution networks," *International Journal of Electrical Power & Energy Systems*, vol. 94, pp. 141–150, 2018.

[21] A. Yaramasu, Y. Cao, G. Liu, and B. Wu, "Aircraft electric system intermittent arc fault detection and location," *IEEE Transactions on Aerospace and Electronic Systems*, vol. 51, no. 1, pp. 40–51, 2015.

[22] N. L. Georgijevic, M. V. Jankovic, S. Srdic, and Z. Radakovic, "The detection of series arc fault in photovoltaic systems based on the arc current entropy," *IEEE Transactions on Power Electronics*, vol. 31, no. 8, pp. 5917–5930, 2016.

[23] G. Artale, A. Cataliotti, V. Cosentino, D. Di Cara, S. Nuccio, and G. Tine, "Arc fault detection method based on CZT low-frequency harmonic current analysis," *IEEE Transactions on Instrumentation and Measurement*, vol. 66, no. 5, pp. 888–896, 2017.

[24] Z. Hameed and K. Wang, "Clustring analysis to improve the reliability and maintainability of wind turbines with self-organizing map neural network," *International Journal of Performability Engineering*, vol. 9, no. 3, pp. 245–260, 2013.

[25] Y. W. Zhang, T. Xiang, and X. Guo, "Service quality prediction based on SOM neural network," *Journal of Software*, vol. 29, no. 11, pp. 3388–3399, 2018.

[26] B. Q. Yin, Y. G. He, and Y. Q. Zhu, "A power quality multi-disturbance detection and recognition method based on generalized transform and fuzzy SOM network," *Chinese Society for Electrical Engineering*, vol. 35, no. 4, pp. 866–872, 2015.

[27] S. D. Dai, W. Z. Ju, and K. W. Xia, "Optimized design of low energy consumption for low voltage circuit breakers using PSO algorithm," *Journal of Electro-technics*, vol. 32, no. 19, pp. 100–106, 2017.

[28] M. N. Tang, S. J. Chen, X. H. Zheng, T. Wang, and H. Cao, "Sensors deployment optimization in multi-dimensional space based on improved particle swarm optimization algorithm," *Journal of Systems Engineering and Electronics*, vol. 29, no. 5, pp. 969–982, 2018.

[29] Y. X. Xie, T. Q. Liu, and X. N. Su, "Feature selection of transient stability assessment based on distributed particle swarm optimization algorithm in hadoop architecture," *Power Grid Technology*, vol. 42, no. 12, pp. 4107–4115, 2018.

[30] D. G. Peng, Y. W. Chen, and Y. L. Qian, "Soft-measurement model of transformer winding temperature based on particle swarm optimization-support vector regression," *Transmission of China ElectroTech*, vol. 33, no. 8, pp. 1742–1761, 2018.

[31] L. Y. Zhou, L. X. Ding, and H. Peng, "A particle swarm optimization algorithm for inverse center of gravity center learning," *Journal of Electronics*, vol. 45, no. 11, pp. 2815–2824, 2017.

[32] C. L. Zhou, Z. S. Qian, and Q. M. Wang, "Identification and reduction of power line conducted leakage signal based on PSO-SVM method," *Journal of Electronic & Information Technology*, vol. 40, no. 9, pp. 2206–2211, 2018.